



Photodynamic Inactivation of *Botrytis cinerea* Spores by Curcumin—Effect of Treatment Factors and Characterization of Photo-generated Reactive Oxygen Species

Maral Seididamyeh¹ · Michael E. Netzel¹ · Ram Mereddy² · Jeffrey R. Harmer³ · Yasmina Sultanbawa¹

Received: 24 March 2023 / Accepted: 19 June 2023 / Published online: 5 July 2023
© The Author(s) 2023

Abstract

Botrytis cinerea is the main cause of gray mold in a wide range of fresh produce, which causes huge losses in pre- and/or post-harvest stages and is therefore considered the second major plant pathogen globally. Since the application of synthetic fungicides is not allowed in postharvest conditions, alternative natural approaches are required to reduce the resulting spoilage. The aim of this study was to investigate the efficacy of photodynamic treatment in inactivating *B. cinerea* spores in vitro, for which the interactive effect of influential treatment parameters on curcumin phototoxicity was studied using an I-optimal design. Results showed that the antifungal activity of the treatment was significantly dependent on solvent, curcumin concentration, and irradiance, except for light dose. A complete photoinactivation of spores was obtained in an aqueous ethanolic environment (optimum condition: 13 μM , 31.75 mW cm^{-2} , 19.05 J cm^{-2}), compared to when curcumin was dissolved in medium-chain-triglyceride (MCT) oil. Furthermore, the photogeneration of superoxide anion and hydroxyl radicals was demonstrated by electron paramagnetic resonance spectroscopy, which indicates the occurrence of a type-I photodynamic reaction. These findings suggest that curcumin-based photosensitization can inhibit/reduce fungal infection, which can be employed in pre/post-harvest stages to reduce the waste caused by spoilage.

Keywords Electron paramagnetic resonance spectroscopy · Fungal spores · Photodynamic inactivation · Visible light

Introduction

Botrytis cinerea, the phytopathogenic fungus, is the main cause of gray mold in a wide range of fresh produce such as grapes, blueberries, eggplants, pepper, tomatoes, and strawberries (Elad et al., 2016). The infection can occur on several parts of the plant, including stem, flowers, leaves, seeds, and fruits, at different plant growth stages, starting from seedling to fruit ripening and even during storage and transportation

(Dean et al., 2012). The broad range of host species and the huge losses in pre- and/or post-harvest stages make it the second major plant pathogen globally (Dean et al., 2012), and it is classified as a high-risk pathogen. Annual losses of \$10 billion to \$100 billion have been estimated for *Botrytis* diseases worldwide (Boddy, 2016). To control the *B. cinerea* infection, synthetic fungicides are applied on the field, which has been considered a fairly safe approach for plant protection. Nevertheless, pathogen resistance development, the potential risks of the residuals to consumer health, and environmental impacts are considered the main concerns of fungicide application on crops. Therefore, the food industry is in dire need of a green and sustainable alternative measure to control and reduce the incidence of *B. cinerea* infection in fresh produce during both production and postharvest storage and distribution.

Photodynamic treatment, also known as photosensitization, is one of the recently introduced decontamination technologies in the food industry. It consists of the illumination of a photosensitizer with light of an appropriate wavelength. This leads to the excitation of the photosensitizer,

✉ Yasmina Sultanbawa
y.sultanbawa@uq.edu.au

¹ ARC Industrial Transformation Training Centre for Uniquely Australian Foods, Centre for Nutrition and Food Sciences, Queensland Alliance for Agriculture and Food Innovation, The University of Queensland, Indooroopilly, QLD 4068, Australia

² Department of Agriculture and Fisheries, Queensland Government, Coopers Plains, QLD 4108, Australia

³ The Centre for Advanced Imaging, The University of Queensland, QLD 4072 St. Lucia, Australia

resulting in the generation of cytotoxic reactive oxygen species (ROS) such as hydroxyl, superoxide anion, and singlet oxygen. These, in turn, interact with the cellular structures of microorganisms (i.e., lipid membrane, proteins, and nucleic acids), causing oxidative cellular damage and ending up in cell death (Baltazar et al., 2015). These photodynamically generated short-lived radical species can be indirectly studied by electron paramagnetic resonance (EPR) spectroscopy coupled with the spin-trapping technique. This is facilitated by stable, paramagnetic EPR-detectable spin adducts that are generated by spin-trapping of short-lived radicals such as hydroxyl (OH^\bullet) and superoxide anion ($\text{O}_2^{\bullet-}$) via addition to the double bond of nitron or nitroso compounds (i.e., diamagnetic spin traps) (Villamena & Zweier, 2004). The paramagnetic characteristic of spin adducts allows them to be detectable by EPR and exhibit spectra with specific hyperfine splitting constants and g -value parameters of the trapped free radical (Rosen et al., 1999). The successful application of DMPO and PBN as trapping reagents for reactive oxygen species as well as producing persistent spin adducts has been demonstrated in the literature (Ferreira et al., 2017; Gonçalves et al., 2020). DMPO and PBN are nitron spin traps in which the α -position carbon, relative to the nitrogen, scavenges the free radical species (Rosen et al., 1999). Generally, photodynamic treatment enjoys the advantages of low-energy requirement, no toxic chemical usage, flexibility of application for various purposes (e.g., microbial inactivation on the surface of food, packaging material, and food processing equipment), and no observed microbial resistance to the treatment (Penha et al., 2017).

Curcumin, the flavonoid isolated from the *Curcuma longa* roots, is a naturally occurring photosensitizer with maximum absorption at ca. 420 nm (i.e., blue light) with a penetration depth of hardly 1 mm (Clement et al., 2009) and high cell membrane permeability (Sun et al., 2008). Therefore, it is suitable for surface decontamination of food products with less adverse impact on the nutritional and chemical composition of the treated foods. Moreover, curcumin is recognized as safe to be consumed according to the Food and Drug Administration (FDA) of the USA because of its low toxicity (FDA, 2016). The phototoxicity of curcumin against a broad range of microorganisms such as Gram-positive bacteria, Gram-negative bacteria, viruses, yeasts, and molds has been studied, and a promising inactivation efficiency was reported (Al-Asmari et al., 2017; Chen et al., 2020; Nima et al., 2021). However, the interactive effects of treatment parameters on the phototoxicity of curcumin have not been studied, for which response surface methodology (RSM) was employed. RSM is widely used to study the relationship between factors (i.e., independent variables) and the investigating responses (i.e., dependent variables), as well as the inter-interaction of factors, which allows the simultaneous optimization of multiple factors (Myers et al.,

2016). Therefore, this study looks at an I-optimal design of the curcumin formulations in different solvents and their in vitro phototoxicity against *B. cinerea* spores, the isolated microorganism from Australian-grown strawberries (Seidi Damyeh et al., 2021), at different illumination conditions. This probes the main factors affecting the photoinactivation efficiency of curcumin (viz., solvent, curcumin concentration, irradiance, and light dose), which was the primary goal of this study. Furthermore, the EPR-spin trapping technique was employed to characterize the amount and type of photogenerated ROS.

Materials and Methods

Design of Experiments

Randomized RSM was used to generate an I-optimal quadratic design (Design Expert, v.11.1.2.0, Stat-Ease, Minneapolis, MN, USA) to investigate the effect of curcumin concentration (13–130 μM), light dose (19.05–66.53 J cm^{-2}), irradiance (31.75–44.35 mW cm^{-2}), and solvent (ethanol, medium chain triglyceride (MCT) oil, ethanol-MCT) on the antimicrobial photodynamic activity of curcumin against *B. cinerea* spores by studying log reduction and viability of spores as dependent variables (Table 1). Since curcumin is sparingly soluble in water, the effect of solvent on the phototoxicity of curcumin was also considered. The levels of the independent variables were determined based on preliminary experiments to achieve acceptable antimicrobial activity (data not shown). The actual variables were coded to aid the multiple regression analysis.

Preparation of Curcumin Solutions

Curcumin (from *Curcuma longa*, $\geq 65\%$, Sigma-Aldrich, St Louis, MO, USA) stock solutions were prepared in three solvents, namely ethanol (99.8%, Fisher Chemical, Loughborough, UK), MCT oil (derived from coconut oil (C8, C10), 100%, Melrose, Mt Waverley, VIC, Australia), and ethanol-MCT oil mixture (1:1, v/v), and were kept at -20°C until analysis. The purity of curcumin was considered in calculating the curcumin concentration in the final solutions. Ultrapure water (Milli-Q, Millipore, Burlington, MA, USA) was added to the respective stock solutions to have a 5% curcumin-solvent phase in the final working solutions (v/v). Tween 80 (Polyoxyethylene (20) sorbitan mono-oleate, BDH Chemicals, Kilsyth, VIC, Australia) was added to the solutions containing MCT oil as a surfactant to achieve a homogeneous solution. This was followed by vortexing the solutions for 5 min at 3000 rpm (Heathrow Scientific, Vernon Hills, IL, USA). The prepared solutions were kept at 4°C for 2 days.

Table 1 I-optimal quadratic design with the observed correspondent responses (i.e., log reduction and cell viability)

Run	A ^a	B ^b	C ^c	D ^d	Log ₁₀ CFU ml ⁻¹ reduction	Cell viability (%)
1	91	42.79	31.75	Ethanol	0.79	65.20
2	91	42.79	38.57	Ethanol	4.00	4.06
3	13	19.05	31.75	Ethanol	4.00	5.61
4	52	19.05	31.75	MCT	0.42	37.86
5	130	42.79	31.75	Ethanol-MCT	0.65	42.36
6	130	19.05	44.35	Ethanol-MCT	0.65	43.94
7	52	42.79	31.75	Ethanol-MCT	1.33	42.54
8	130	42.79	38.57	MCT	0.29	38.08
9	52	66.53	44.35	MCT	0.98	42.03
10	52	42.79	44.35	Ethanol	4.00	0.93
11	13	66.53	31.75	Ethanol-MCT	0.76	41.94
12	52	19.05	38.57	Ethanol-MCT	0.87	54.38
13	130	19.05	38.57	Ethanol	0.86	76.21
14	91	19.05	44.35	MCT	0.91	40.72
15	13	42.79	31.75	MCT	0.32	38.23
16	13	42.79	44.35	Ethanol-MCT	0.90	36.48
17	91	66.53	38.57	Ethanol-MCT	1.17	27.94
18	130	42.79	38.57	MCT	0.00	49.88
19	130	19.05	31.75	MCT	0.17	43.86
20	130	66.53	31.75	MCT	0.44	48.16
21	52	42.79	44.35	Ethanol	4.00	0.48
22	52	19.05	38.57	Ethanol-MCT	0.93	51.42
23	13	19.05	44.35	MCT	0.95	36.05
24	13	66.53	38.57	Ethanol	4.00	6.09
25	91	19.05	31.75	Ethanol-MCT	0.89	41.84
26	130	66.53	44.35	Ethanol	4.00	11.82
27	91	42.79	31.75	Ethanol	0.73	49.35
28	91	66.53	38.57	Ethanol-MCT	0.58	42.04
29	13	66.53	38.57	Ethanol	3.34	1.27
30	52	66.53	31.75	MCT	0.19	43.15

^aCurcumin concentration (μM)^bLight dose (J cm⁻²)^cIrradiance (mW cm⁻²)^dSolvent

Absorbance and Fluorescence Spectra

UV–visible and fluorescence spectra of curcumin solutions (13, 52, 91, and 130 μM) were recorded with a spectrophotometer (Varioskan LUX 3020–80,884, Thermo Scientific, Singapore). The absorbance spectra were recorded within the wavelength range of 300–700- and 1-nm steps. The fluorescence emission spectra were acquired by exciting samples at 430 nm, which corresponds to the curcumin maximum absorption wavelength. The slit width was set at 1 nm and the spectra were recorded from 450 to 750 nm. All these measurements were carried out on freshly made solutions in triplicate and at room temperature.

Spore Suspension

The asexual spores of *B. cinerea* are conidia and responsible for easy transmission of the infection and were targeted in this work. The isolated *B. cinerea* from the commercial strawberry cultivar ‘Red Rhapsody’ grown in Queensland, Australia (Seidi Damyeh et al., 2021) was cultured at 25 °C on potato dextrose agar (CM0139, Oxoid, Basingstoke, Hampshire, UK). Spores were harvested from a 2-week-old culture by gently rubbing the surface flooded with sterile, ultrapure water, followed by filtering with a 2-layer sterile cheesecloth. The filtrate was centrifuged (4500 × g, 4 °C; 5804 R centrifuge, Eppendorf, Hamburg,

Germany), washed with sterile ultrapure water, and centrifuged again. The resulting pellet was resuspended in sterile ultrapure water and counted with a Haemocytometer. The spore suspension was then kept at 4 °C and was used within a week.

Phototoxicity in Suspension Culture

To study the phototoxicity effect of curcumin solutions on the growth and viability of the spores, a 10^4 CFU ml⁻¹ concentration of spore suspension was prepared in sterile ultrapure water and potato dextrose broth (PDB; Sigma-Aldrich, St Louis, MO, USA). Samples were prepared in sterile 96-well plates by adding 50 µl of curcumin solution and 50 µl of spore suspension. This was followed by illumination under LED light (420 nm, 200 W, 100–240 V; COB LED Light Fixture, HYG05-4, China) for the given time (Table 1). The photosynthetic photon flux density (PPFD) of LEDs was measured using a spectrometer (HR-450, HiPoint, Kaohsiung, Taiwan) at 10 different positions at a 10-cm distance from the light source. PPFD (µmol m⁻² s⁻¹) was converted to light irradiance (mW cm⁻²) by the following formula (Roh et al., 2016):

$$\text{Light irradiance (mW cm}^{-2}\text{)} = \frac{h \times C \times A \times \text{PPFD} \times 10^4}{\lambda}$$

where h is Planck's constant (6.63×10^{-34} J s⁻¹), C is the light velocity (3×10^8 m s⁻¹), A is the Avogadro constant (6.022×10^{23} photon mol⁻¹), and λ is the wavelength (nm).

The dark control samples were incubated for 10 min in darkness at room temperature in the presence of different curcumin formulations. For a negative control representing 0 µM of curcumin, sterile ultrapure water, or PDB, was added.

Effect of Photosensitization on the *B. cinerea* Growth

To facilitate the *B. cinerea* colony counting, a selective medium was prepared according to the method given by Edwards and Seddon (2001). Aliquots of 30 µl were taken from the homogenized treated samples, spread-plated on *Botrytis* selective media, and incubated at 25 °C for 4 days. The number of viable colonies was then counted (colony counter, Stuart Scientific, Staffordshire, UK) and recorded as a Log₁₀ (CFU ml⁻¹) reduction.

Effect of Photosensitization on *B. cinerea* Viability

Tetrazolium dye (MTT) assay was used to evaluate the survival rate of the spores (Shamali et al., 2018). This assay measures the colored formazans produced through the

reduction of colorless tetrazolium salts, which is an indication of the proliferation and viability of microbial cells (Stentelaire et al., 2001). After 24-h incubation at 25 °C, 10 µl of aqueous MTT solution (5 mg ml⁻¹; EMD Millipore Group, Darmstadt, Germany) was added to each sample, mixed properly, and kept at 25 °C in an incubator for 2 h. The media were then removed, and 200 µl dimethyl sulfoxide (Sigma-Aldrich) was added, mixed, and incubated overnight at 25 °C to enhance the formazan dissolution. The fungal plug was then removed, and absorbance was read at 570 nm (Infinite M200, Tecan GmbH, Grödig, Austria). The viability was calculated as below:

$$\text{Viability(\%)} = \frac{\text{Absorbance of treated spore} - \text{Absorbance of MTT in DMSO}}{\text{Absorbance of the untreated spore} - \text{Absorbance of MTT in DMSO}} \times 100$$

Electron Paramagnetic Resonance Spectroscopy

A spin-trapping electron paramagnetic resonance (EPR) protocol was applied to detect, identify, and measure the ROS produced in the curcumin solutions during direct illumination in an X-band continuous wave (CW) EPR cavity (Fig. S.1) for 15 min at 440 nm using two different light irradiances (43.59 and 62.71 mW cm⁻²). EPR spectra were recorded with an ELEXSYS EPR spectrometer (Bruker, Rheinstetten, Germany) operated at 9.87 GHz, using a borosilicate glass capillary tube (Kimble Chase, Gerresheimer, Mexico). To detect the produced ROS, 5,5-dimethyl-pyrroline N-oxide (DMPO; 80 mM; > 97%, Chem-Supply, Gillman, SA, Australia) and alpha-phenyl N-tertiary-butyl nitron (PBN; 80 mM; ≥ 98%, Sigma-Aldrich) dissolved in 50% ethanol were used as spin traps for hydroxyl (OH•) and superoxide (O₂•⁻) radicals. Equal aliquots of the spin trap solution and the curcumin solution were mixed, which was used to determine the ROS photogeneration. The EPR signal intensity was recorded during 15 min illumination. Experimental parameters used for EPR operating in X-band were a modulation frequency of 100 kHz, microwave power of 19.82 mW, microwave frequency of ca. 9.87 GHz, a central field of 3518 G, sweep width of 110 G, sweep time of 41.94 s, a modulation frequency of 100 kHz, and a modulation amplitude of 3 G. All the EPR measurements were conducted at room temperature and in triplicate. The EPR spectra of the control samples (i.e., without curcumin) under illumination and the curcumin solutions under darkness were also recorded.

The concentration of photogenerated spin adducts was determined by double integration of the EPR spectrum using MATLAB software (R2020b, MathWorks Inc., Natick, MA, USA) based on known concentrations of ethanolic 4-hydroxy-2,2,6,6-tetramethyl-1-piperidinyloxy radical (TEMPO, 98%; Fujifilm Wako, Japan). Simulation and

fitting of the experimental EPR spectra were performed using the garlic function of the EasySpin toolbox (MATLAB). This resulted in optimized spin-Hamiltonian parameters of the individual spin adducts, and subsequently, concentrations of the total adduct and identified radical adducts were determined from the EPR parameter by comparison to known literature values. The following parameters were used to simulate the PBN-hydroxyl radical adduct: $a_N = 15.5$ G, $a_H = 2.75$ G (Monteiro et al., 2016); DPMO-hydroxyl adduct: $a_N = 15$ G, $a_H = 14.9$ G (Lloyd et al., 1997); DMPO-superoxide anion adduct: $a_N = 14.2$ G, $a_H^\beta = 11.34$ G, $a_H^\gamma = 1.25$ G (Mottley et al., 1986); DMPO radical: $a_N = 14.6$ G (Della Rocca et al., 2021); and DMPO-C₅H₅O₂ adduct: $a_N = 15.8$ G, $a_H = 22.3$ G (Dodd & Jha, 2011).

Statistical Analysis

The analysis of the experimental data was performed by multiple regression analysis using the Design Expert v.11.1.2.0 software. The linear and quadratic effects of independent variables and their interactions involved in the model were analyzed by analysis of variance (ANOVA) at 95% level of confidence ($p \leq 0.05$). To avoid multicollinearity in the models (due to the probable strong correlation of predictors), the stepwise regression procedure (2FI, Quadratic, Reduced Quadratic, and Linear) was applied. The adequacy of the model was determined by the adjusted coefficient of determination (R^2) analysis and lack-of-fit test. The precision of each model tested was evaluated by comparing the obtained responses with the predicted ones from the fitted model. The surface responses were plotted based on the fitted polynomial regression equations to visualize the relationship between variables and responses. Maximizing log reduction and minimizing cell viability were the constraints to optimizing the photosensitization condition, which was validated by conducting four experiments.

Results and Discussion

Absorption Spectra and Fluorescence Emission Spectra of Curcumin

The visible absorption and fluorescence emission spectra for curcumin were measured in different aqueous environments and are presented in the Supplementary Material (Fig. S.2). Significant solvent-dependent shifts in maxima were observed in both spectra. The absorption maxima of curcumin were in the range of 410 to 430 nm, which is in line with previous studies (Santezi et al., 2021; Tsaplev et al., 2020). As shown in Fig. S.2a–c, increasing the curcumin concentration to 130 μ M gave rise to a higher absorbance intensity in the three studied environments. Moreover, a

slightly wider maximum absorbance was observed in aqueous ethanolic environments. For the fluorescence emission, the maxima were at around 560 nm in 13 μ M curcumin in an aqueous ethanolic environment and increasing the concentration to 130 μ M led to a slight “redshift” in the emission maxima to about 570 nm. However, the presence of MCT oil in the environment gave rise to a “blueshift” in the maximum emission at 500 nm (Fig. S.2d–f) with notably stronger fluorescence intensity. However, the lower fluorescence intensity in aqueous ethanolic environments can be related to the self-quenching phenomenon due to more aggregate formation of curcumin in low viscous environments (Iwaki et al., 1993). Therefore, we suggest that less intermolecular collision of curcumin molecules in viscous MCT-containing environments enhances fluorescence intensity, which can, in turn, improve ROS generation.

Effect of Treatment Factors on In Vitro Photoinactivation of *B. cinerea* Spores

The antifungal photodynamic activity of curcumin as a photosensitizer against *B. cinerea* spores is presented in Table 1, and the interactive effect of independent variables on the antifungal activity is reported in the Supplementary data (Tables S.2 and S.3; Figs. S.3 and S.4). The results showed that curcumin-mediated photodynamic treatment was able to inactivate *B. cinerea* spores at the in vitro level (Table 1). There was a considerable variation in the values of log reduction in *B. cinerea* spores' survival (0.19–4.0 \log_{10} (CFU ml^{-1})) as well as their viability (0.48–65.20%) across the various photodynamic conditions. The antimicrobial mechanism of photodynamic treatment is ascribed to the photochemical reactions that trigger upon activation of the photosensitizer by illumination and give rise to ROS generation. These ROS in turn interact non-specifically with various cellular components such as cell walls, cell membranes, enzymes, and DNA (D'Souza et al., 2015) and consequently cause fungal cell death. Wei et al. (2021) reported the occurrence of shrinkage and leakage in *B. cinerea* spores, deformations in cellular organelles, and complete destruction of the nucleus and mitochondria after curcumin-mediated photodynamic treatment (500 μ M, 5 min). The authors maintained that the main photoinactivation mechanism is the ROS damage to the vital cellular components such as the nucleus and mitochondria, while the cell shape and size remained almost intact after the treatment (Wei et al., 2021). Another study on *Penicillium expansum* also showed severe damage to mycelia's cell wall and membrane after curcumin-mediated photodynamic treatment. They observed the vacuolization occurrence on the cell walls using a lower curcumin concentration (30 μ M), while increasing the concentration to 300 μ M led to ruptures in the mycelia's structures (Pang et al., 2022). Neither curcumin nor light alone

showed a significant antifungal effect under the given experimental conditions, affirming that the combination of light and curcumin is necessary for the antifungal photodynamic treatment of *B. cinerea* spores.

A 2-factor interaction (2FI) model was selected to fit the experimental data (Tables S.2 and S.3) as it exhibited the highest R^2 values with a non-significant lack-of-fit value. Results demonstrated the significant ($p < 0.05$) effect of three independent variables (solvent, curcumin concentration, and irradiance) on the antifungal activity of the treatment, whereas light dose showed to be insignificant ($p > 0.05$) (Tables S.2 and S.3). Comparing the F -values, solvent showed the greatest impact on phototoxicity of curcumin, followed by irradiance and curcumin concentration, and light dose exhibited the lowest impact in the studied range (Tables S.2 and S.3). In fact, the solvent can affect the photosensitizer's affinity for the microbial cells via electrostatic and hydrophobic interactions, which are mainly ruled by the surface properties of spore cells such as hydrophobicity and surface charge (Dunlap et al., 2005). This in turn influences the adhesion of the photosensitizer to the microbial cell and, consequently, the antifungal photodynamic inactivation. Furthermore, irradiance and the concentration of photosensitizer can affect the quantum yield and the half-life of the triplet excited state (Spikes, 1989), which directly impacts the efficiency of treatment.

Figure 1 and Fig. S.5 and S.6 exhibit the three-dimensional surface plots of log reduction and cell viability as a function of independent variables at three different levels. Surface plots enabled the visualization of the interactive effects and interdependency of the four investigated variables. The higher photo-decontamination ability of curcumin was observed in aqueous ethanolic solution (Fig. 1), compared to aqueous MCT and ethanol-MCT environments (Figs. S.5 and S.6). The investigated variables and their interactions showed no significant ($p > 0.05$) effect on the antifungal photodynamic activity of curcumin in aqueous MCT and ethanol-MCT solutions (Fig. S.6a–f). Under all experimental conditions, when MCT-containing formulations were used, the viability of *B. cinerea* was reduced to 27.94–54.38%. The limited phototoxicity of curcumin in MCT oil-contained environments could be attributed to the encapsulation of most curcumin molecules in oil droplets as well as the low affinity of the spore hydrophobic cell wall to the lipophilic droplets containing curcumin. Therefore, curcumin may show a higher affinity for the core of emulsion droplets than the spore's outer surface, and the probability of photoperoxidation of the emulsion droplets seems to be greater than the damage to spore cells. The free curcumin present in the MCT-containing environments could then contribute to the observed low antifungal effect of the treatment.

On the other hand, curcumin demonstrated a higher antifungal photodynamic activity in the aqueous ethanolic

environments, which enabled a complete reduction in the survival of *B. cinerea* spores ($4 \log_{10}$ (CFU ml⁻¹)) (Table 1). The photochemical properties of curcumin and therefore its phototoxicity are substantially affected by the H-binding capacity of the environment (Chignell et al., 1994). It is possible that curcumin forms a complex with the outer surface of *B. cinerea* spores, which is induced by electrostatic interactions and/or H-bond formation in the hydrogen bond donating and accepting solvents such as ethanol. In fact, the phenolic OH group in the curcumin structure accepts hydrogen from the solvent or outer surface of microorganisms (Tønnesen, 2006). This encourages better adhesion of the photosensitizer to the spores and therefore results in better photoinactivation efficiency. Moreover, antifungal inactivation was shown to be affected by curcumin concentration and light irradiance. When the light irradiance was maintained constant at the central value, reducing curcumin concentration and light dose resulted in improved photocontamination of *B. cinerea* spores in aqueous ethanolic environments (Fig. 1a). A similar trend was observed when the light dose was maintained constant and higher antifungal activity was achieved by decreasing the curcumin concentration, even though higher light irradiance was desirable for obtaining higher photoinduced death of fungal spores in higher curcumin concentrations, as shown in Fig. 1c–f, which was demonstrated by higher log reduction and lower spore viability. This could be attributed to the poor solubility of curcumin in aqueous environments, which consequently tends to aggregate in higher concentrations. This in turn has an adverse effect on not only the light absorption and excitation phenomenon but also its attachment to microbial cells (Konan et al., 2002), which contributes to the antimicrobial photodynamic activity of curcumin. Our results are in contrast with those reported in the literature, where the conventional step-by-step approach was used, and therefore the possible interactions between factors could not be studied. For example, Song et al. (2020) observed that increasing light dose led to an increase in curcumin phototoxicity against *P. expansum* spores, while they observed no significant differences between different curcumin concentrations (50–500 μ M). In another study, complete inactivation of *Listeria monocytogenes* was obtained by adding 1 μ M of curcumin to an aqueous ethanolic solution. The authors found that the photoinactivation ability of curcumin was enhanced by increasing the light dose (Huang et al., 2020).

This study optimized the curcumin-mediated photosensitization condition for four investigated variables, namely curcumin concentration, light dose, irradiance, and solvent to obtain higher phototoxicity of curcumin, as indicated by higher log reduction and lower viability. The optimized condition of curcumin-mediated photosensitization was 13 μ M of aqueous ethanolic curcumin with illumination at

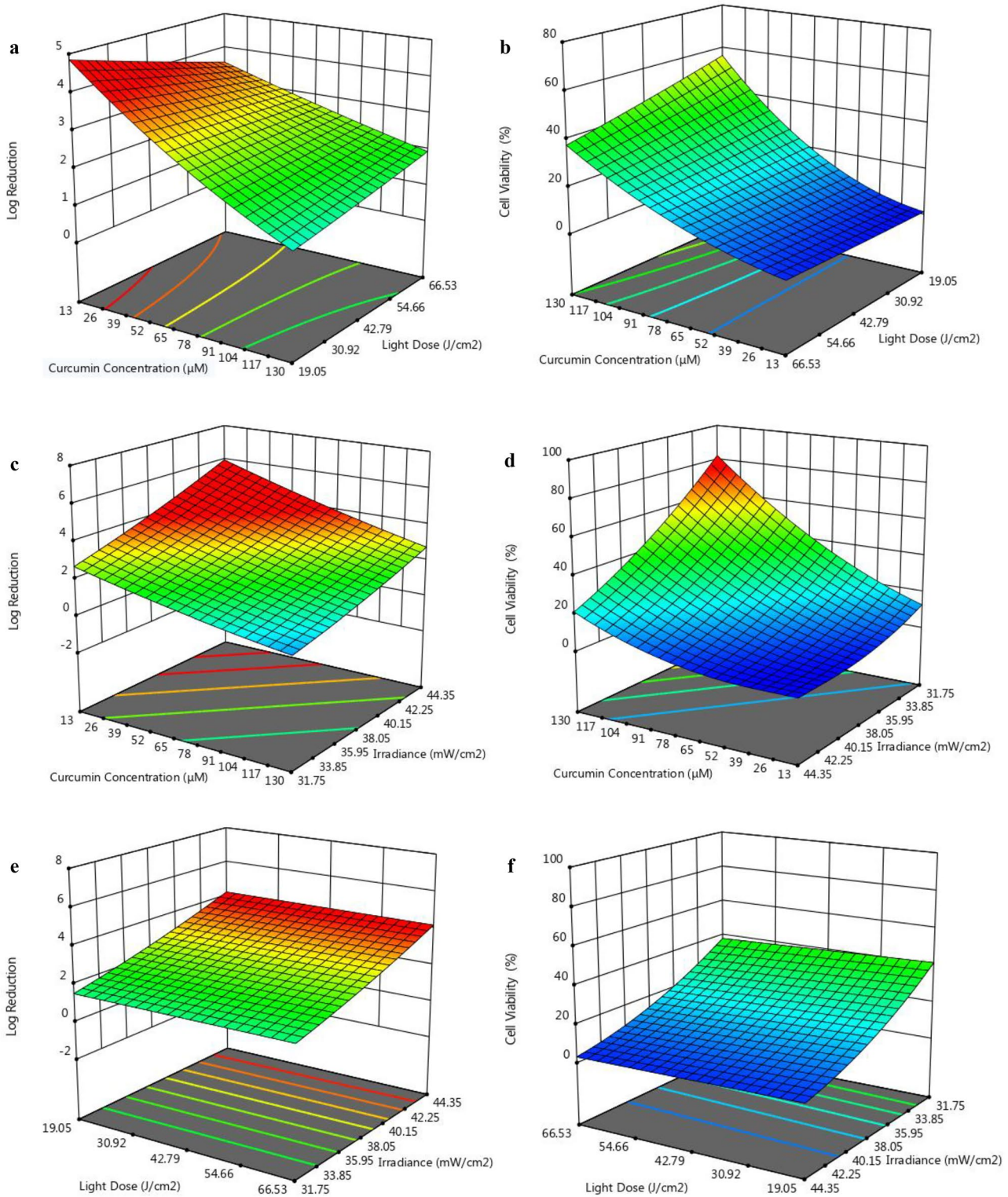


Fig. 1 Surface graphs of different interaction effects in the aqueous ethanolic environment: curcumin concentration and light dose on **a** *Botrytis cinerea* log reduction ($\log(\text{CFU ml}^{-1})$) and **b** cell viability at a constant irradiance of 38.05 mW cm^{-2} ; curcumin concentration and irradiance on **c** log reduction and **d** cell viability at a con-

stant light dose of 42.79 J cm^{-2} ; light dose and irradiance on **e** log reduction and **f** cell viability at a constant curcumin concentration of $71.50 \mu\text{M}$ (color scale: log reduction 0 [blue] 4 [red], cell viability 0.475947 [blue] 76.2111 [red])

31.75 mW cm⁻² and 19.05 J cm⁻². A 3.25 Log (CFU ml⁻¹) reduction and 7.65% spore viability were obtained under the optimized condition, which was in agreement with the predicted values of 3.25 log (CFU ml⁻¹) and 9.91%, respectively. This in turn confirms the reliability of the optimized photosensitization condition, which is recommended for further application.

Generation and Evolution of Radicals (O₂^{•-} and OH[•])

The photoexcitation of curcumin under the given experimental conditions led to the gradual generation of EPR spectra upon continuous illumination in the presence of a spin trap (i.e., DMPO or PBN). This dynamic process of trapping is presented in the Supplementary Material (Figs. S.7–S.12). It was shown that the signal intensity of DMPO and PBN adducts in the aqueous ethanolic environment is directly proportional to curcumin concentration, irradiance, and illumination time. A substantial rise in the characteristic quartet-line signal of DMPO and the six-line signal of PBN adducts was obtained by increasing the curcumin concentration and irradiance (Figs. S.7 and S.8, respectively). The MCT oil-containing formulations, on the other hand, were only studied at an irradiance of 62.71 mW cm⁻² and in the presence of DMPO. Similarly, an increase in curcumin concentration

enhanced the EPR signal intensity (Figs. S.11 and S.12). Figure 2 shows the evolution of experimental and simulated EPR spectra for DMPO and PBN adducts over the 15-min illumination. Compared to the PBN spectra, more intense and complex EPR spectra were obtained in the presence of DMPO. The simulation of the spectra according to the literature (Della Rocca et al., 2021; Dodd & Jha, 2011; Monteiro et al., 2016) revealed that four spin adducts, including DMPO-OH[•], DMPO-O₂^{•-}, DMPO-OC₂H₅[•], and DMPO[•], contributed to the obtained experimental EPR spectra with the partially overlapped spectra (Fig. 2a–c).

The variation in concentrations of total ROS and the identified radical adducts as a function of illumination time in different curcumin formulations at 43.59 and 62.71 mWcm⁻² using DMPO and PBN as the spin trap is illustrated in Figs. 3, 4, and 5. The generation of ROS showed distinct patterns under different experimental conditions. Generally, three phases of ROS generation can be observed, as shown in Fig. 3. The first quantities of ROS generated are represented by a sharp line gradient (the first phase), which indicates the activation of readily accessible curcumin molecules in the environment (Figs. 3 and 5). As can be seen in Figs. 3–5, the starting time of ROS generation was rough once the illumination started. This demonstrates the instant light energy take-up by the curcumin

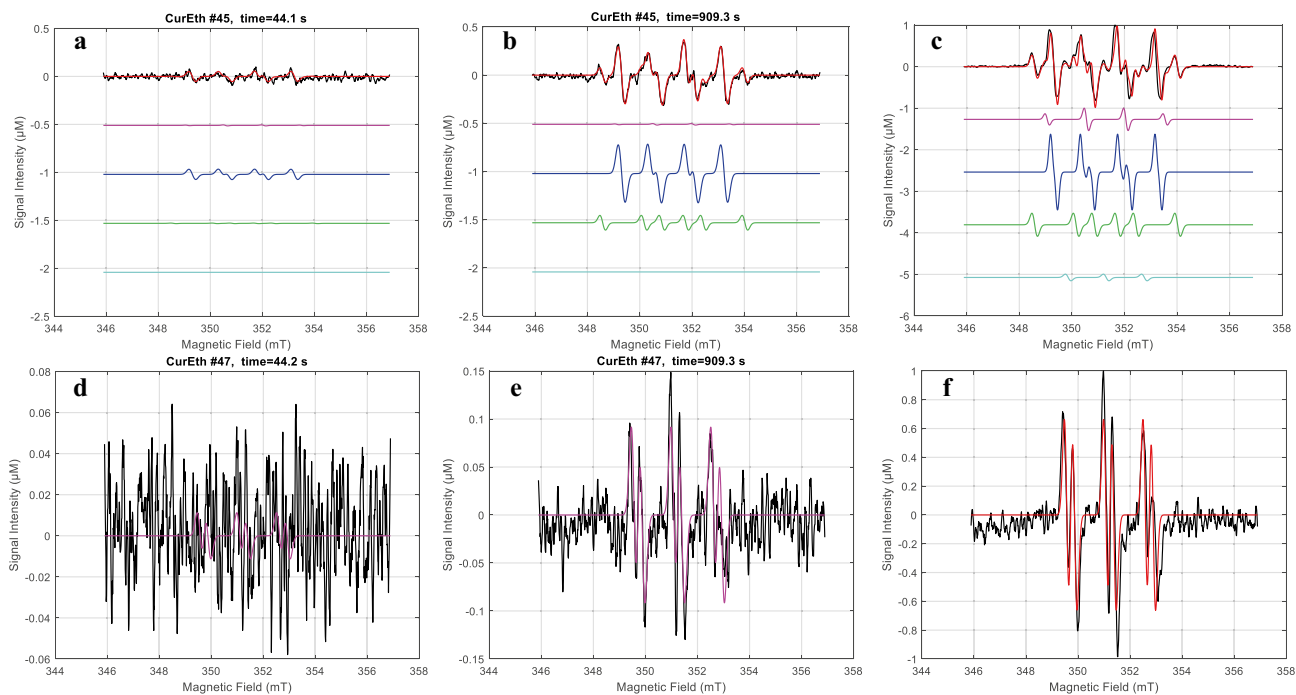


Fig. 2 Experimental (black line) and simulated EPR spectra (red line) for aqueous ethanolic curcumin solutions (91 µM, 15 min illumination at 43.59 mW cm⁻²): DMPO-ROS adducts after 44.2 s illumination (a), after 909.3 s illumination (b), and the average of 15 min illumination (c) including DMPO-hydroxyl adduct (magenta), DMPO-superoxide

anion adduct (blue), DMPO-hydroxyethyl adduct (green), and DMPO radical (cyan); PBN-ROS adducts after 44.2 s illumination (d), after 909.3 s illumination (e), and the average of 15 min illumination (f) including PBN-hydroxyl adduct (magenta)

molecules (< 30 s) to be excited and therefore rapid ROS generation in photodynamic treatment. This is followed by the second increasing phase with a slower rate, which indicates that the ROS generation is nearing completion. This phase was however observed in aqueous ethanolic environments only (Fig. 3), which probably represents the duration needed to level up the energy of curcumin molecules entrapped in the self-formed aggregates—due to curcumin insolubility in water—to their excitation point.

On the other hand, the first phase of ROS generation is indicated by a steeper upward line in MCT-contained environments (Fig. 5) that reached the maximal amount of generated ROS (6.46 μM (Fig. 5a) and 8.19 μM (Fig. 5b) in a considerably shorter time. This was followed by a sharp fall, indicating the completion of ROS generation. This can be due to the greater homogeneity of curcumin in these environments compared to aqueous ethanolic solutions, where curcumin shows a higher tendency to aggregate. The third stage in ROS generation is almost plateau, which demonstrates the least quantity of ROS is generated by the few amounts of curcumin molecules left in the environment and therefore yield is roughly constant with time (Fig. 3). This is where either there are no more curcumin molecules to be excited or the whole system has come to some kind of equilibrium that marks the end of the ROS generation process, which is then followed by a reducing slope. Nevertheless, only the first phase was observed for hydroxyl generation when PBN was used as the spin trap (Fig. 4). This can suggest that either there was enough PBN in the environment to react with the continuously generated hydroxyl radicals during the illumination or that the high stability of PBN-OH adducts led to their detection for a longer time. Furthermore, this shows that the applied illumination condition did not promote photolytic decay of the generated adducts.

The photogeneration of ROS was shown to be directly proportional to curcumin concentration as well as light intensity (Figs. 3–5). The latter, which was only studied in aqueous ethanolic environments, could contribute to the rapid activation of curcumin molecules and therefore reach the end of ROS generation faster (Fig. 3b). It was also shown that ROS generation in terms of DMPO and PBN adducts increased by 1.5 and 2 times, respectively, when the irradiance was increased from 43.59 to 62.71 mW cm^{-2} . Moreover, a considerably low (< 1 μM) amount of spin adducts (i.e., ROS) was detected at the lowest curcumin concentration (13 μM) in aqueous ethanolic environments. However, this was increased by 12 times in an aqueous ethanolic environments and by 4 times in MCT-contained environments when the highest curcumin concentration (130 μM) was used (Figs. 3 and 5). Using PBN also showed a rise in photogeneration of spin adducts by increasing curcumin concentration from 13 to 91 μM ; however, further increases

in concentration did not improve the ROS generation at the two studied irradiances (Fig. 4a, b).

The simulation and identification of the radicals that contributed to the observed total ROS, demonstrated that $\text{O}_2^{\bullet-}$ (superoxide anion) rather than $\bullet\text{OH}$ (hydroxyl) was the dominant photodynamically generated ROS in the studied curcumin environments (Figs. 3–5). The efficacy and rate of $\text{O}_2^{\bullet-}$ trapping by DMPO are affected by a number of environmental factors, such as solvent (Villamena, 2016). The author also suggested that a high concentration of DMPO is required for $\text{O}_2^{\bullet-}$ trapping. Thus, 40 mM of DMPO used in this study could result in more efficient $\text{O}_2^{\bullet-}$ trapping, as indicated by stronger DMPO- O_2^{\bullet} adduct signals (Fig. 2; reaction (3)). The observed rapid decay of EPR signals for the MCT-contained environments is possibly due to the high instability of DMPO- O_2^{\bullet} adducts ($\tau_{1/2} = 60$ s) (Tuccio et al., 1995), which was sufficient for the time frame of our measurements to detect the adduct. Therefore, we suggest that either there was not enough spin trap in the environment to react with the high amounts of generated ROS, or the observed spin-adduct concentration was the maximal amount that curcumin molecules in the environment could produce. The observed signal decay could also be caused by the radical scavenging ability of MCT oil containing lauric acid, caprylic acid, and caproic acid with reported antiradical (i.e., antioxidant) activity (Oh & Shahidi, 2018). In this case, we suggest that there might be a competitive environment between MCT oil and DMPO to react with the generated ROS, in which MCT oil seems to be more successful in scavenging the radicals. The signal decay could also have occurred due to the oxygen deficiency in the reaction environment, indicating the oxygen dependency of type I photosensitization. It should be mentioned that the control experiments showed no OH^{\bullet} and $\text{O}_2^{\bullet-}$ generation in aqueous MCT solutions without curcumin. This result is in accordance with the in vitro results against *B. cinerea* spores.

The observed low-intensity signals of DMPO-OH adduct (reaction (4)) could be attributed to the inhibitory effect of ethanol toward DMPO-OH formation by scavenging the $\bullet\text{OH}$ radicals and generating hydroxyethyl radicals (reaction (5)) (Ergaieg et al., 2008), which has also been reported in the Fenton system (Finkelstein et al., 1980). This reaction was confirmed by the slight increase in the concentration of DMPO- OC_2H_5 adducts during the 15-min illumination in all investigated environments (Figs. 3 and 5c–j). Therefore, higher concentrations of DMPO are required for comparable amounts of $\bullet\text{OH}$ radicals to react with both spin trap and ethanol and, in turn, to enable the detection of DMPO-OH adducts (Andersen & Skibsted, 1998). Furthermore, the possible formation of DMPO-OH from DMPO-OOH (resulting from DMPO- O_2^{\bullet}) can be ruled out since the DMPO-OH signal did not rise with the decay of DMPO- O_2^{\bullet} . This is in accordance with the findings of Finkelstein et al. (1982) and

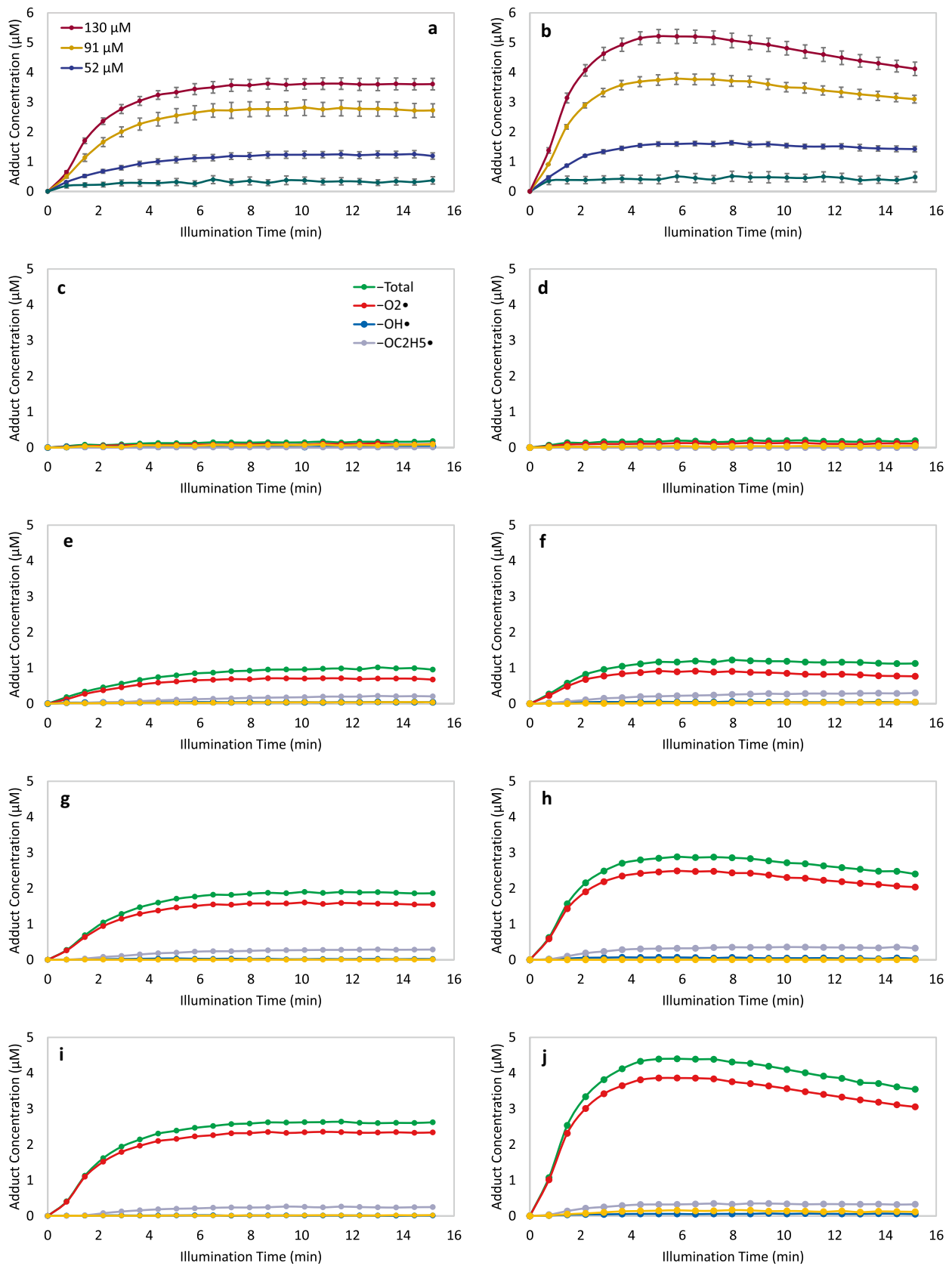


Fig. 3 Evolution of total (experimental) adduct and simulated and fitted radical adduct concentration (μM) over 15 min illumination of different concentrations of curcumin in aqueous ethanolic solutions using DMPO as spin trap, **a** total radical adduct formation at 43.59 mW cm^{-2} , **b** total radical adduct (μM) formation at 62.71 mW cm^{-2} , **c** $13 \mu\text{M}$ curcumin at 43.59 mW cm^{-2} , **d** $13 \mu\text{M}$ curcumin at 62.71 mW cm^{-2} , **e** $52 \mu\text{M}$ curcumin at 43.59 mW cm^{-2} , **f** $52 \mu\text{M}$ curcumin at 62.71 mW cm^{-2} , **g** $91 \mu\text{M}$ curcumin at 43.59 mW cm^{-2} , **h** $91 \mu\text{M}$ curcumin at 62.71 mW cm^{-2} , **i** $130 \mu\text{M}$ curcumin at 43.59 mW cm^{-2} , and **j** $130 \mu\text{M}$ curcumin at 62.71 mW cm^{-2} . The results are the mean of at least three replicates. The error bar indicates the standard error of at least three replicates

Buettner (1990) that less than 3% of DMPO-OOH converts into DMPO-OH. Using PBN as a spin trap, on the other hand, enabled us to detect the photogeneration of hydroxyl radicals in the studied curcumin environments (Fig. 4c, d). The six-line EPR spectrum observed arises from the coupling of the electron spin to the nuclear spins of the ^{14}N ($I=1$) and ^1H (H_{β} , $I=1/2$) nuclei of the spin trap with characteristic hyperfine coupling values for a PBN-OH adduct (Buettner, 1987). These data thus reveal that $\bullet\text{OH}$ radicals are being generated. No other EPR signals of PBN adducts with other ROS were detected, which might be due to the high instability of other adducts or the higher efficacy of PBN in trapping $\bullet\text{OH}$ radicals.

It should be noted that prior to illumination, a small multicomponent paramagnetic signal attributed to DMPO \bullet

and DMPO-OC $_2\text{H}_5$ was detected in all samples containing DMPO and ethanol. The detection of DMPO-OC $_2\text{H}_5$ adducts in the absence of light or curcumin is attributed to the reaction between ethanol and DMPO that results in the formation of ethoxy radicals by hydrogen abstraction from ethanol (Brezová et al., 2004), which also leads to the generation of DMPO-OC $_2\text{H}_5$ (reaction (6)) adducts. The fourth identified DMPO adduct resulted from the degradation of DMPO molecules through their protonation (Della Rocca et al., 2021), and therefore DMPO \bullet adducts were also observed within the multicomponent spectra (reactions (7) and (8); Fig. 2c). In the absence of light or curcumin, the two main components of photosensitization, no EPR signal relative to the OH \bullet and O $_2^{\bullet-}$ adducts was observed (data not shown), indicating that the ROS formation is a photodynamic process.

Probable Mechanisms

From the EPR spin-trapping spectroscopy, a powerful tool to study short-lived radicals, it was concluded that the superoxide anion was the dominant ROS generated through photoexcitation of curcumin in different environments. Therefore, it is speculated that the continual generation of mainly superoxide anion in aqueous ethanolic solutions of curcumin leads to its observed phototoxicity against *B. cinerea*. The possible mechanism can be the

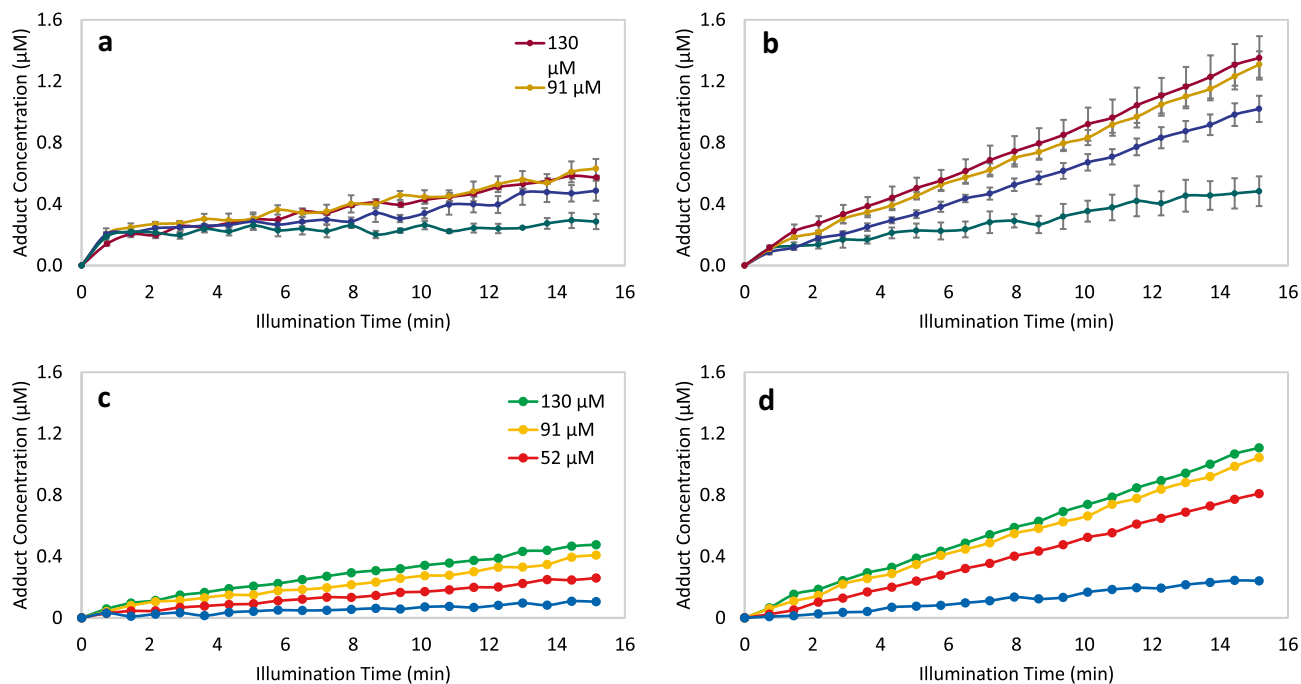


Fig. 4 Evolution of total (experimental) adduct and simulated and fitted radical ($\bullet\text{OH}$) adduct concentration (μM) over 15 min illumination of different concentrations of curcumin in aqueous ethanolic solutions using PBN as a spin trap. Total radical-adduct concentration at **a**

43.59 mW cm^{-2} and **b** 62.71 mW cm^{-2} ; fitted PBN- $\bullet\text{OH}$ adduct concentration at **c** 43.59 mW cm^{-2} and **d** 62.71 mW cm^{-2} . The results are the mean of at least three replicates. The error bar indicates the standard error of at least three replicates

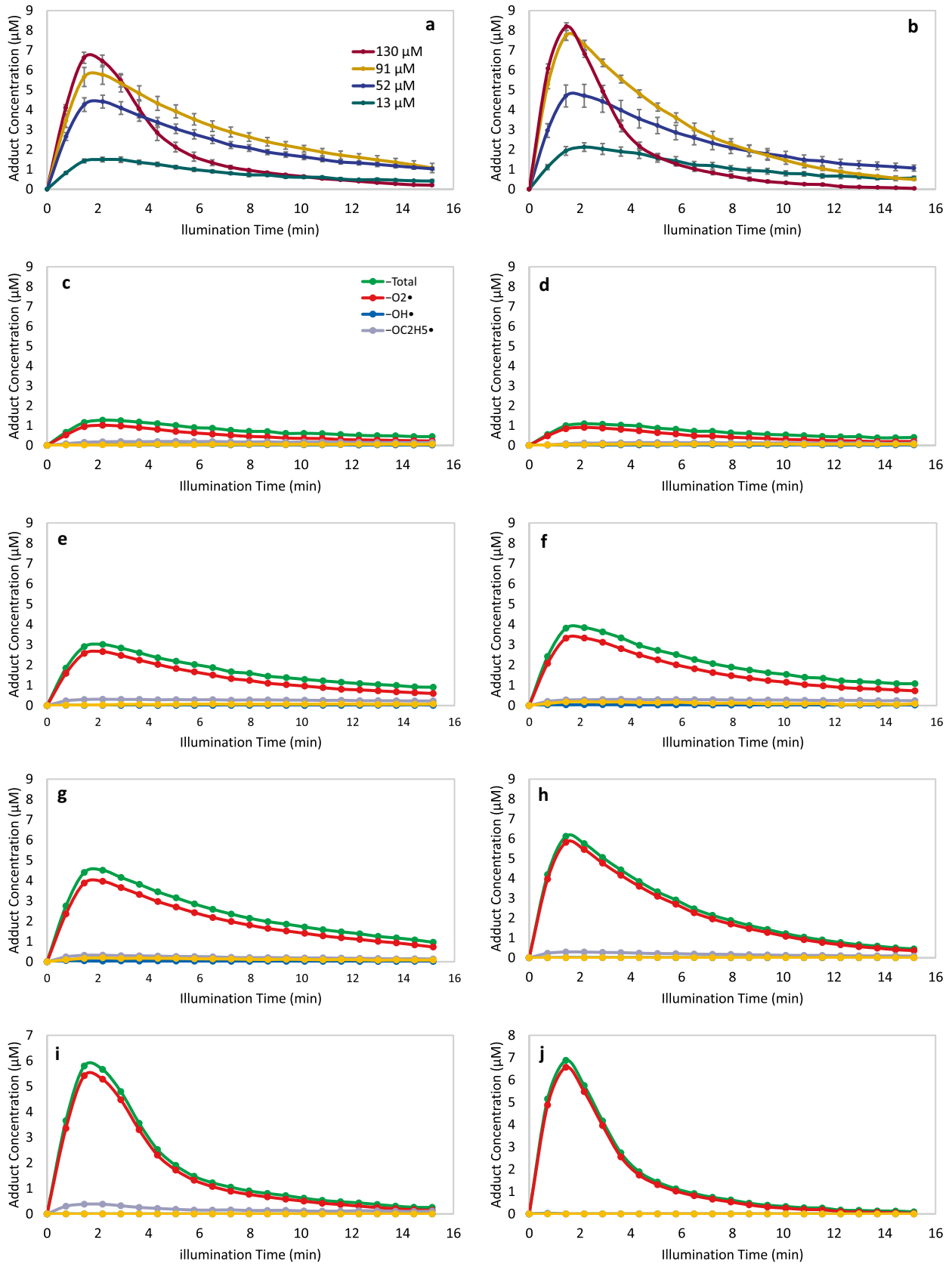
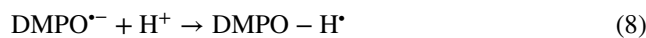
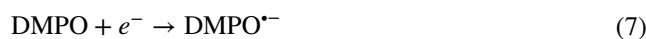
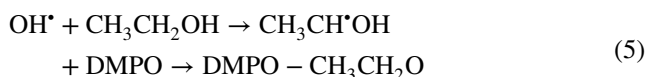
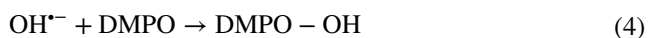
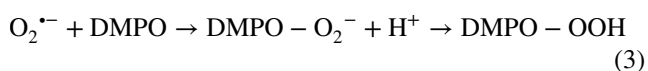
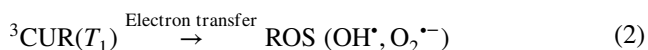
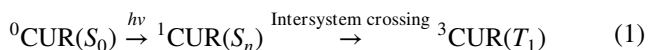


Fig. 5 Evolution of total (experimental) adduct and simulated and fitted radical adduct concentration (μM) over 15 min illumination of different concentrations of curcumin, dissolved in aqueous solutions of MCT oil and mixture of MCT and ethanol (MCT-Eth), at 62.71 mW cm^{-2} using DMPO as spin trap, **a** total radical adduct formation, MCT; **b** total radical adduct formation, MCT-Eth; **c** $13 \mu\text{M}$ curcumin, MCT; **d** $13 \mu\text{M}$ curcumin, MCT-Eth; **e** $52 \mu\text{M}$ curcumin, MCT; **f** $52 \mu\text{M}$ curcumin, MCT-Eth; **g** $91 \mu\text{M}$ curcumin, MCT; **h** $91 \mu\text{M}$ curcumin, MCT-Eth; **i** $130 \mu\text{M}$ curcumin, MCT; and **j** $130 \mu\text{M}$ curcumin, MCT-Eth. The results are the mean of at least three replicates. The error bar indicates the standard error of at least three replicates

activation of curcumin molecules (S_0) by visible light, i.e., photoexcitation, resulting in an unstable singlet excited state (S_n), which is converted to a long-lived triplet state (T_1) through intersystem crossing. The generated triplet state then undergoes two different pathways (type I or II) to produce cytotoxic ROS. Hydroxyl and superoxide anion are the results of the type I mechanism by transferring electrons to dissolved oxygen molecules, followed by their reduction. While a collision between the triplet state and the ground state oxygen molecule leads to an energy transfer to oxygen, producing singlet oxygen through the type II mechanism (DeRosa & Crutchley, 2002), notwithstanding this, electron transfer from an electron donor such as a photosensitizer molecule can result in singlet oxygen reduction and conversion into a superoxide anion, which has been reported in biological systems (Peters & Rodgers, 1980). To clarify the origin of the observed superoxide anion in the curcumin solutions, further studies are recommended using specific ROS inhibitors such as beta-carotene for $^1\text{O}_2$ and superoxide dismutase for $\text{O}_2^{\bullet-}$ to study and measure one radical at a time. Overall, the generation of $\text{O}_2^{\bullet-}$ and OH^\bullet indicates the photodynamic activity of curcumin in the studied solvents. The mechanism of photosensitization of curcumin (CUR) and radical spin-trapping reactions can be described as follows:



The spin-trapping reaction between radical (R^\bullet) and trap (T) is generally described by a second-order reaction that results in a spin-adduct ([SA]) formation. The amount of generated R^\bullet is reflected in the spin-adduct concentration (SA) if spin trapping is the only reaction to take place. Therefore, the rate of R^\bullet formation (F) is equal to the rate of spin-adduct formation. Nevertheless, the instability of spin adducts leads to their decay to EPR-silent products (P) at either an equal or higher rate (D , decay rate) than the spin-adduct formation rate. In general, the observed changes in spin-adduct concentration over illumination time can be due to spin-adduct formation and spin-adduct decay in the absence of other possible reactions (11).

$$F = \frac{dR^\bullet}{dt} = \frac{d[\text{SA}]}{dt} \quad (9)$$



$$\frac{d[\text{SA}]}{dt} = F - D \quad (11)$$

The spin-adduct decay is affected by the environment, such as the concentration of the spin trap (Roubaud et al., 1997). To find out the actual amount of trapped ROS upon illumination, we need to also study the decay process of spin-adducts in the absence of light, which was not performed in this study. Furthermore, spin trapping is not the only reaction that ROS undergoes. There are many other chemical reactions that the highly reactive free radicals easily participate in to form EPR silent products (XR). This in turn influences the spin-trapping efficiency (E), which can be described as the ratio of the spin-adduct formation rate to the rate of all other reactions (V_i) and free radical formation (13).



$$E = \frac{\frac{d[\text{SA}]}{dt}}{V_i + F} \quad (13)$$

Calculating trapping efficiency could become complicated if any reaction involved in V_i is other than a first-order one, leading to efficiency changes over time. Furthermore, the radical trapping process and achieving the actual spin-adduct concentration become more complicated if spin-adducts rapidly decompose by reacting with the surrounding free radicals, such as DMPO-OH adduct decay caused by a superoxide anion.

Conclusion

In this study, curcumin-based photodecontamination conditions were optimized using RSM, which enabled us to study the interactions between the factors influencing the photosensitization treatment. Among the studied curcumin formulations, aqueous ethanolic solutions showed a higher efficiency in *B. cinerea* photoinactivation. The concentration and irradiance dependency of curcumin phototoxicity were also investigated. Furthermore, the photodynamic generation of ROS in different curcumin aqueous environments was determined by EPR spectroscopy. The occurrence of type I photodynamic reaction was demonstrated by identifying OH^\bullet and $\text{O}_2^{\bullet-}$ radicals during the curcumin-based photosensitization. However, further studies are needed to elucidate the potential singlet oxygen generation, indicating a type II pathway of photodynamic reaction.

Supplementary Information The online version contains supplementary material available at <https://doi.org/10.1007/s11947-023-03150-w>.

Acknowledgements The authors thank Margaret Currie and Andrew Cusack (Department of Agriculture and Fisheries, QLD, Australia) for their technical support.

Author Contribution Maral Seididamyeh (M.S.): conceptualization, methodology, investigation, formal analysis, and writing—original draft. Michael E. Netzel (M.E.N.): supervision and writing—review and editing. Ram Mereddy (R.M.): supervision and writing—review and editing. Jeffrey R. Harmer (J.R.H.): methodology and writing—review and editing. Yasmina Sultanbawa (Y.S.): supervision, resources, funding acquisition, and writing—review and editing.

Funding Open Access funding enabled and organized by CAUL and its Member Institutions. Maral Seididamyeh acknowledges the support from the Australian Government via the Research Training Program Scholarship for her doctorate studies at the University of Queensland (Brisbane, QLD, Australia). This work was supported by Horticulture Innovation Australia Limited (HN15001 Naturally Nutritious Project) and the Australian Research Council's (ARC) Industrial Transformation Training Centre (ITTC) for Uniquely Australian Foods (Grant number: IC180100045).

Data Availability The datasets generated during and/or analyzed during the current study are available from the corresponding author upon reasonable request.

Declarations

Conflict of Interest The authors declare no conflict of interest.

Open Access This article is licensed under a Creative Commons Attribution 4.0 International License, which permits use, sharing, adaptation, distribution and reproduction in any medium or format, as long as you give appropriate credit to the original author(s) and the source, provide a link to the Creative Commons licence, and indicate if changes were made. The images or other third party material in this article are included in the article's Creative Commons licence, unless indicated otherwise in a credit line to the material. If material is not included in the article's Creative Commons licence and your intended use is not permitted by statutory regulation or exceeds the permitted use, you will

need to obtain permission directly from the copyright holder. To view a copy of this licence, visit <http://creativecommons.org/licenses/by/4.0/>.

References

- Al-Asmari, F., Mereddy, R., & Sultanbawa, Y. (2017). A novel photosensitization treatment for the inactivation of fungal spores and cells mediated by curcumin. *Journal of Photochemistry and Photobiology b: Biology*, *173*, 301–306.
- Andersen, M. L., & Skibsted, L. H. (1998). Electron spin resonance spin trapping identification of radicals formed during aerobic forced aging of beer. *Journal of Agricultural and Food Chemistry*, *46*(4), 1272–1275.
- Baltazar, L. M., Ray, A., Santos, D. A., Cisalpino, P. S., Friedman, A. J., & Nosanchuk, J. D. (2015). Antimicrobial photodynamic therapy: An effective alternative approach to control fungal infections. *Frontiers in Microbiology*, *6*, 202.
- Boddy, L. (2016). Pathogens of autotrophs. In S. C. Watkinson, L. Boddy, & N. P. Money (Eds.), *The Fungi* (pp. 245–292). Elsevier.
- Brezová, V., Pigošová, J., & Havlínová, B., Dvoranová, D., & Ďurovič, M. (2004). EPR study of photochemical transformations of triarylmethane dyes. *Dyes and Pigments*, *61*(2), 177–198.
- Buettner, G. R. (1987). Spin Trapping: ESR parameters of spin adducts 1474 1528V. *Free Radical Biology and Medicine*, *3*(4), 259–303.
- Buettner, G. R. (1990). Ascorbate oxidation: UV absorbance of ascorbate and ESR spectroscopy of the ascorbyl radical as assays for iron. *Free Radical Research Communications*, *10*(1–2), 5–9.
- Chen, B., Huang, J., Li, H., Zeng, Q.-H., Wang, J. J., Liu, H., Pan, Y., & Zhao, Y. (2020). Eradication of planktonic *Vibrio parahaemolyticus* and its sessile biofilm by curcumin-mediated photodynamic inactivation. *Food Control*, *113*, 107181.
- Chignell, C. F., Bilski, P., Reszka, K. J., Motten, A. G., Sik, R. H., & Dahl, T. A. (1994). Spectral and photochemical properties of curcumin. *Photochemistry and Photobiology*, *59*, 295–302.
- Clement, M., Daniel, G., & Trelles, M. (2009). Optimising the design of a broad-band light source for the treatment of skin. *Journal of Cosmetic and Laser Therapy*, *7*, 177–189.
- D'Souza, C., Yuk, H. G., Khoo, G. H., & Zhou, W. (2015). Application of light-emitting diodes in food production, postharvest preservation, and microbiological food safety. *Comprehensive Reviews in Food Science and Food Safety*, *14*(6), 719–740.
- Dean, R., Van Kan, J. A., Pretorius, Z. A., Hammond-Kosack, K. E., Di Pietro, A., Spanu, P. D., Rudd, J. J., Dickman, M., Kahmann, R., & Ellis, J. (2012). The Top 10 fungal pathogens in molecular plant pathology. *Molecular Plant Pathology*, *13*(4), 414–430.
- Della Rocca, D. G., Victoria, H. F., Moura-Nickel, C. D., Scaratti, G., Krambrock, K., De Noni, A., Vilar, V. J., Jose, H. J., & Moreira, R. F. (2021). Peroxidation and photo-peroxidation of pantoprazole in aqueous solution using silver molybdate as catalyst. *Chemosphere*, *262*, 127671.
- DeRosa, M. C., & Crutchley, R. J. (2002). Photosensitized singlet oxygen and its applications. *Coordination Chemistry Reviews*, *233*, 351–371.
- Dodd, N. J., & Jha, A. N. (2011). Photoexcitation of aqueous suspensions of titanium dioxide nanoparticles: An electron spin resonance spin trapping study of potentially oxidative reactions. *Photochemistry and Photobiology*, *87*(3), 632–640.
- Dunlap, C. A., Biresaw, G., & Jackson, M. A. (2005). Hydrophobic and electrostatic cell surface properties of blastospores of the entomopathogenic fungus *Paecilomyces fumosoroseus*. *Colloids and Surfaces b: Biointerfaces*, *46*(4), 261–266.
- Edwards, S., & Seddon, B. (2001). Selective media for the specific isolation and enumeration of *Botrytis cinerea* conidia. *Letters in Applied Microbiology*, *32*(2), 63–66.

- Elad, Y., Vivier, M., & Fillinger, S. (2016). *Botrytis*, the good, the bad and the ugly. In S. Fillinger & Y. Elad (Eds.), *Botrytis-the fungus, the pathogen and its management in agricultural systems* (pp. 1–15). Springer.
- Ergaieg, K., Chevanne, M., Cillard, J., & Seux, R. (2008). Involvement of both type I and type II mechanisms in Gram-positive and Gram-negative bacteria photosensitization by a meso-substituted cationic porphyrin. *Solar Energy*, 82(12), 1107–1117.
- FDA. (2016). Summary of safety data and food usage conditions for conclusion of general recognition of safety of BCM-95 (curcumin). *Food and Drug Administration*, L. Dolcas Biotech.
- Ferreira, D. C., Monteiro, C. S., Chaves, C. R., Sáfar, G. A., Moreira, R. L., Pinheiro, M. V., Martins, D. C., Ladeira, L. O., & Krambrock, K. (2017). Hybrid systems based on gold nanostructures and porphyrins as promising photosensitizers for photodynamic therapy. *Colloids and Surfaces b: Biointerfaces*, 150, 297–307.
- Finkelstein, E., Rosen, G. M., & Rauckman, E. J. (1980). Spin trapping of superoxide and hydroxyl radical: Practical aspects. *Archives of Biochemistry and Biophysics*, 200(1), 1–16.
- Finkelstein, E., Rosen, G. M., & Rauckman, E. J. (1982). Production of hydroxyl radical by decomposition of superoxide spin-trapped adducts. *Molecular Pharmacology*, 21(2), 262–265.
- Gonçalves, P. J., Bezzerra, F. C., Teles, A. V., Menezes, L. B., Alves, K. M., Alonso, L., Alonso, A., Andrade, M. A., Borissevitch, I. E., & Souza, G. R. (2020). Photoinactivation of *Salmonella enterica* (serovar Typhimurium) by tetra-cationic porphyrins containing peripheral [Ru (bpy) 2Cl]+ units. *Journal of Photochemistry and Photobiology a: Chemistry*, 391, 112375.
- Huang, J., Chen, B., Li, H., Zeng, Q.-H., Wang, J. J., Liu, H., Pan, Y., & Zhao, Y. (2020). Enhanced antibacterial and antibiofilm functions of the curcumin-mediated photodynamic inactivation against *Listeria monocytogenes*. *Food Control*, 108, 106886.
- Iwaki, T., Torigoe, C., Noji, M., & Nakanishi, M. (1993). Antibodies for fluorescent molecular rotors. *Biochemistry*, 32(29), 7589–7592.
- Konan, Y. N., Gurny, R., & Allémann, E. (2002). State of the art in the delivery of photosensitizers for photodynamic therapy. *Journal of Photochemistry and Photobiology b: Biology*, 66(2), 89–106.
- Lloyd, R. V., Hanna, P. M., & Mason, R. P. (1997). The origin of the hydroxyl radical oxygen in the Fenton reaction. *Free Radical Biology and Medicine*, 22(5), 885–888.
- Monteiro, C. S., Ferreira, D. C., Sáfar, G. A., Gontijo, R. N., Fantini, C., Martins, D. C., Idemori, Y. M., Pinheiro, M. V., & Krambrock, K. (2016). Unravelling the mechanisms of reactive oxygen species formation in nanohybrid systems of porphyrins and enriched (6, 5) single-walled carbon nanotubes for photosensitization. *Physical Chemistry Chemical Physics*, 18(30), 20459–20465.
- Mottley, C., Connor, H. D., & Mason, R. P. (1986). [¹⁷O]oxygen hyperfine structure for the hydroxyl and superoxide radical adducts of the spin traps DMPO, PBN and 4-POBN. *Biochemical and Biophysical Research Communications*, 141(2), 622–628.
- Myers, R. H., Montgomery, D. C., & Anderson-Cook, C. M. (2016). *Response surface methodology: Process and product optimization using designed experiments*. John Wiley & Sons.
- Nima, G., Soto-Montero, J., Alves, L. A., Mattos-Graner, R. O., & Giannini, M. (2021). Photodynamic inactivation of *Streptococcus mutans* by curcumin in combination with EDTA. *Dental Materials*, 37(1), e1–e14.
- Oh, W. Y., & Shahidi, F. (2018). Antioxidant activity of resveratrol ester derivatives in food and biological model systems. *Food Chemistry*, 261, 267–273.
- Pang, J., Zhang, F., Wang, Z., Wu, Q., Liu, B., & Meng, X. (2022). Inhibitory effect and mechanism of curcumin-based photodynamic inactivation on patulin secretion by *Penicillium expansum*. *Innovative Food Science and Emerging Technologies*, 80, 103078.
- Penha, C. B., Bonin, E., da Silva, A. F., Hioka, N., Zanqueta, É. B., Nakamura, T. U., de Abreu Filho, B. A., Campanerut-Sá, P. A. Z., & Mikcha, J. M. G. (2017). Photodynamic inactivation of food-borne and food spoilage bacteria by curcumin. *LWT-Food Science and Technology*, 76, 198–202.
- Peters, G., & Rodgers, M. (1980). On the feasibility of electron transfer to singlet oxygen from mitochondrial components. *Biochemical and Biophysical Research Communications*, 96(2), 770–776.
- Roh, H. J., Kim, A., Kang, G. S., & Kim, D.-H. (2016). Photoinactivation of major bacterial pathogens in aquaculture. *Fisheries and Aquatic Sciences*, 19(1), 1–7.
- Rosen, G. M., Britigan, B. E., Halpern, H. J., & Pou, S. (1999). *Free radicals: Biology and detection by spin trapping*. Oxford University Press.
- Roubaud, V., Sankarapandi, S., Kuppasamy, P., Tordo, P., & Zweier, J. L. (1997). Quantitative measurement of superoxide generation using the spin trap 5-(diethoxyphosphoryl)-5-methyl-1-pyrroline-N-oxide. *Analytical Biochemistry*, 247(2), 404–411.
- Santezi, C., Reina, B. D., de Annunzio, S. R., Calixto, G., Chorilli, M., & Dovigo, L. N. (2021). Photodynamic potential of curcumin in bioadhesive formulations: Optical characteristics and antimicrobial effect against biofilms. *Photodiagnosis and Photodynamic Therapy*, 35, 102416.
- Seidi Damyeh, M., Fernando, C. W., Phan, A. D. T., Hong, H. T., Mereddy, R., Netzel, M. E., Chaliha, M., & Sultanbawa, Y. (2021). Post-harvest fungal occurrence on commercial strawberry cultivars grown in Australia: Impact of phytochemical composition. *Journal of Food Measurement and Characterization*, 15, 3811–3822.
- Shamali, N., Preuß, A., Saltsman, I., Mahammed, A., Gross, Z., Däschlein, G., & Röder, B. (2018). In vitro photodynamic inactivation (PDI) of pathogenic germs inducing onychomycosis. *Photodiagnosis and Photodynamic Therapy*, 24, 358–365.
- Song, L., Zhang, F., Yu, J., Wei, C., Han, Q., & Meng, X. (2020). Antifungal effect and possible mechanism of curcumin mediated photodynamic technology against *Penicillium expansum*. *Postharvest Biology and Technology*, 167, 111234.
- Spikes, J.D. (1989). Photosensitization. In K. C. Smith (Ed.), *The science of photobiology* (2nd ed., pp. 79–110). Plenum Press.
- Stentelaire, C., Antoine, N., Cabrol, C., Feron, G., & Durand, A. (2001). Development of a rapid and highly sensitive biochemical method for the measurement of fungal spore viability: An alternative to the CFU method. *Enzyme and Microbial Technology*, 29(8–9), 560–566.
- Sun, Y., Lee, C.-C., Hung, W.-C., Chen, F.-Y., Lee, M.-T., & Huang, H. W. (2008). The bound states of amphipathic drugs in lipid bilayers: Study of curcumin. *Biophysical Journal*, 95(5), 2318–2324.
- Tønnesen, H.H. (2006). Solubility and stability of curcumin in solutions containing alginate and other viscosity modifying macromolecules. *Die Pharmazie – An International Journal of Pharmaceutical Sciences*, 61, 696–700.
- Tsaplev, Y. B., Lapina, V. A., & Trofimov, A. V. (2020). Curcumin in dimethyl sulfoxide: Stability, spectral, luminescent and acid-base properties. *Dyes and Pigments*, 177, 108327.
- Tuccio, B., Lauricella, R., Fréjaville, C., Bouteiller, J.-C., & Tordo, P. (1995). Decay of the hydroperoxyl spin adduct of 5-(diethoxyphosphoryl)-5-methyl-1-pyrroline N-oxide: An EPR kinetic study. *Journal of the Chemical Society, Perkin Transactions*, 2(2), 295–298.
- Villamena, F. A. (2016). *Reactive species detection in biology: From fluorescence to electron paramagnetic resonance spectroscopy*. Elsevier.
- Villamena, F. A., & Zweier, J. L. (2004). Detection of reactive oxygen and nitrogen species by EPR spin trapping. *Antioxidants and Redox Signaling*, 6(3), 619–629.

Wei, C., Zhang, F., Song, L., Chen, X., & Meng, X. (2021). Photosensitization effect of curcumin for controlling plant pathogen *Botrytis cinerea* in postharvest apple. *Food Control*, *123*, 107683.

Publisher's Note Springer Nature remains neutral with regard to jurisdictional claims in published maps and institutional affiliations.